Arch. Min. Sci. **68** (2023), 2, 267-283

Electronic version (in color) of this paper is available: http://mining.archives.pl

DOI: https://doi.org/10.24425/ams.2023.146179

YANG CAO[1*], WANG HONGHONG[1], WANG HAODONG[2,3]

NUMERICAL SIMULATION ON CONSEQUENCES OF GENERATOR FIRE ACCIDENT ON OFFSHORE PLATFORM – A CASE STUDY

The high temperature and thermal radiation caused by generator fire accidents on the offshore platform lead to the destruction of equipment and facilities and threaten the structural safety of the offshore platform. Based on the background of a crude oil generator fire accident on an offshore platform, KFX software was used to conduct a numerical simulation of the fire process and explore the spatial-temporal variation characteristics of smoke, temperature and heat radiation within the scope of the fire room. The influence ranges of 12.5 kW/m^2, 25 kW/m^2 and 35 kW/m^2 were obtained according to the thermal radiation criterion. Researchers examined the temperature variation and heat flow at the room's ceiling and floor near the primary steel support. The results show that: 1) The surface temperatures of partial steel supports exceed 550°C, and the heat flux of partial steel supports exceeds 37.5 kW/m^2. 2) In the ignition position, the maximum temperature at the ceiling reaches 2299°C when t = 24 s, and the maximum temperature at the flooring reaches 701°C when t = 79 s. The heat radiation flux at the ceiling and flooring both exceeds 25 kW/m^2. The maximum temperature of partial crude oil generators can reach 1299°C. 3) The heat radiation flux of partial generators can reach 105 kW/m^2, and the heat radiation flux at the adjacent point of partial generators never exceeds 20 kW/m^2. The above research results can provide a reference for checking the response time of flame detectors and the strength of the supporting structure.

Keywords: offshore platform fires; generator fires; fire damage evaluation; steel structure damage in fires; fire simulation

[1] DEPARTMENT OF ENGINEERING DESIGN AND RESEARCH, CNOOC RESEARCH INSTITUTE CO., LTD. 100028 BEIJING, CHINA

[2] COLLEGE OF SAFETY AND OCEAN ENGINEERING, CHINA UNIVERSITY OF PETROLEUM (BEIJING), BEIJING 102249, CHINA

[3] KEY LABORATORY OF OIL AND GAS SAFETY AND EMERGENCY TECHNOLOGY, MINISTRY OF EMERGENCY MANAGEMENT, BEIJING 102249, CHINA

* Corresponding author: wwwcaoyang@126.com

Introduction

A fire accident caused by generator leakage is one of the most common types of fire accidents on offshore oil and gas platforms, which leads to equipment damage and personnel injury. The adverse products commonly caused by fire are toxic smoke, high temperature and thermal radiation. On the one hand, toxic smoke poses a threat to workers' breathing. On the other hand, it will reduce invisibility and seriously hinder workers from escaping. High temperature or thermal radiation not only brings about high temperature burns, but also causes damage to equipment and steel structures, and even collapse of structures. Therefore, such adverse factors are regarded as the important indexes considered in the design and evaluation for the safety of offshore oil and gas platforms [1-4].

At present, lots of relevant studies are carried out in China or overseas. For instance, Guo Jie [5] simulated and analysed the fire of crude oil leakage in the oil and gas processing system on an offshore platform, and determined the best evacuation path through a comparative analysis of thermal radiation intensity and temperature of different escape stairways. Chen Changyun [6] studied the law of smoke spread and diffusion of fire in the main engine cabin and lower deck, and analysed its impact on personnel evacuation safety. Tong Fei et al. [7] based on FDS and ABAQUS, studied the structural thermal response of offshore platform rooms under the coupling action of non-uniform temperature field and wave load under local fire. Niu Tianxin [8] studied the flame morphology characteristics, temperature field and heat radiation flux distribution of FPSO superstructure pool fire under different wind speeds. Based on numerical simulation, Yoon et al. [9] studied the influence of fire heat source, wind speed, wind direction and other factors on thermal diffusion behaviour in the upper module area of FPSO. Xie Xiulong [10] carried out a fire risk analysis of the FPSO pump cabin and studied the change characteristics of thermal radiation, temperature and smoke layer height with and without fire fighting.

The generator, installed on an offshore platform, acts as an important role in providing electricity for daily running. It consumes various fuels, like crude oil, diesel or natural gas, which are all easily ignited. On January 20, 2015, a generator's engine caught fire due to a backbreaking fuel gas leak caused by the spark of the exhaust pipe. On January 18, 2020, the engine of the generator caught fire because the fuel intake hose burst and crude oil spewed into the outer cover of the high-temperature exhaust pipe. It is found that high temperatures caused by fire may lead to irreversible deformation of steel structure, reduce its strength, and affect the structural safety of offshore platforms locally or as a whole [11]. The radiant heat generated by a fire will also damage equipment and facilities, which may produce new leakage and lead to further expansion of fire accidents [12]. Generator fire, like a typical fire accident, will cause a series of impacts on the surroundings, which might trigger irreversible damage to adjacent objects. It is essential to know the temperatures of the room structure around the burning generator, which can be used for further analysis of structural loss. It is also important to see the intensity of thermal radiation not only in the fire centre but also from adjacent objects in the room, which impacts personal injury and equipment damage. In this article, a real generator fire was analysed using the numerical simulation method to determine the temperature and thermal radiation characteristics of neighbouring objects.

1. Fire Theory

The flow and heat transfer processes and combustion processes in fire simulation obey the law of conservation of mass, momentum, composition and energy. According to the characteristics of fire combustion in a tank, the general control equation is established as shown in Equation (1) [13]:

$$\frac{\partial(\rho\phi)}{\partial t}+\frac{\partial}{\partial x}(\rho u\phi)+\frac{\partial}{\partial x}(\rho v\phi)+\frac{\partial}{\partial x}(\rho i\phi)= \frac{\partial}{\partial x}\left(\Gamma_\phi\frac{\partial\phi}{\partial x}\right)+\frac{\partial}{\partial y}\left(\Gamma_\phi\frac{\partial\phi}{\partial y}\right)+\frac{\partial}{\partial z}\left(\Gamma_\phi\frac{\partial\phi}{\partial z}\right)+S_\phi \tag{1}$$

Where:

u, v, i — the velocities in x, y, and z directions, m/s;
ρ — the reactant density, kg/m^3;
t — the dimensionless time, s;
ϕ — a general variable, which can represent solution variables such as u, v, T;
Γ_ϕ — the diffusion coefficient, m/s^2;
S_ϕ — the generalised source term.

The eddy dissipation conceptual model (EDC) equation is shown in Equation (2) [13]:

$$\left(\frac{dY_i^*}{dt}\right)+\frac{1}{\tau^*}\left(Y_i^*-Y_i^0\right)=\frac{\omega_i^* W_i}{\rho^*}=R_i^* \qquad \left(\frac{dh^*}{dt}\right)+\frac{1}{\tau^*}\left(h^*-h^0\right)=\left(\frac{1}{\rho^*}\cdot\frac{dP}{dt}\right) \tag{2}$$

Where:

Y_i^* — the mass fraction of component i in the fine structure;
Y_i^0 — the mass fraction of component i outside the reactor;
τ^* — characteristic time scale;
ω^*_i — the reaction rate, kg/(m^2.s);
t — dimensionless time, s;
W — turbulent energy, J/s;
R_i^* — the net formation rate of component i, kg/s;
h^* — the enthalpy in the fine structure, J;
h^0 — the enthalpy outside the reactor, J;
P — the pressure, Pa;
ρ — the reactant density, kg/m^3.

Thermal radiation is calculated using a discrete transmission model proposed by Lockwood and Shah. The model is described by the following formula [14]:

$$I_{n+1}=\frac{\sigma T^4}{\pi}\left(1-e^{-as}\right)+I_n e^{-as} \tag{3}$$

Where:

I_{n+1} and I_n — respectively represent the radiation intensity before and after entering the control body, W/sr;
σ — the radiant heat transfer coefficient, W/(m^2·K);
T — the temperature, K;
a and s — respectively represent the absorption coefficient of the control body and the path distance of the beam.

The amount of radiation propagating between the boundaries can be obtained by integrating the equations in a controlled body one by one along the direction of the ray path. For each surface where radiative heat transfer needs to be calculated, the equation could be established [15]:

$$I_{out} = (1-\varepsilon) I_{in} + \varepsilon\sigma \mathrm{AT}^4 \tag{4}$$

Where:

I_{out} — the intensity of radiation leaving the surface, W/sr;
I_{in} — the intensity of radiation entering the surface, W/sr;
ε — the correction factor;
σ — the radiant heat transfer coefficient, W/(m^2·K);
A — the surface area, m^2;
T — the temperature, K.

2. Engineering Background

2.1. Accident background

The internal dimension of the room for generators is 29 × 28 × 4 m. There are four generators installed inside numbered A, B, C, and D, from the left side. Generators A, B and C are in daily running. Generator D is a spare one. In this case, Generator B got fire because the crude oil was leaking from the inlet hose and spraying the high-temperature exhaust hood at the front end of the turbocharger. Then it gets fired in seconds. The leakage position and ignition position, are shown in Fig. 1.

2.2. Leakage rate calculation

In order to estimate the crude oil leakage rate of the inlet hose, the following formula can be used to calculate [16]:

$$Q_m = C_d A \rho \sqrt{\frac{2(P-P_0)}{\rho}} + 2gh \tag{6}$$

Where:

Q_m — the leakage rate of crude oil, kg/s;
C_d — the crude oil leakage coefficient, taking 0.6;

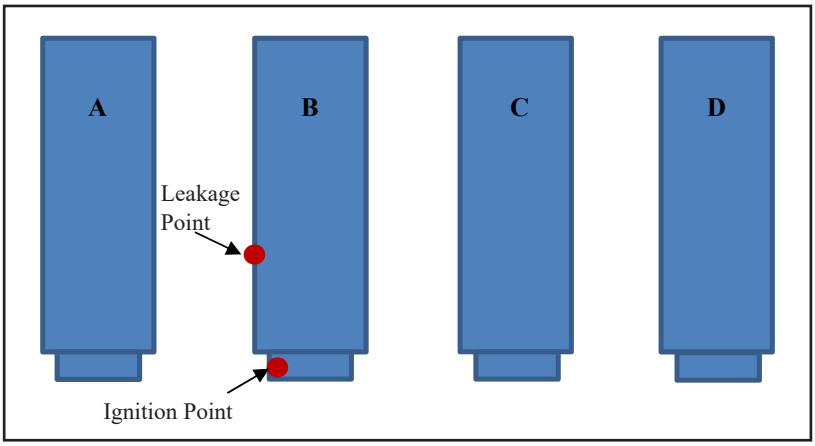

Fig. 1. The floor plan of crude oil generators room

A — the leakage area, m^2, and the shape of the leakage opening is a rectangle with a length of 3 cm and a width of 0.5 cm;
ρ — the density of crude oil, kg/m^3, taking value of 0.885×10^3 kg/m^3;
P — the pressure at the leak of the oil inlet hose, Pa, 3.5×10^6 Pa;
P_0 — the ambient pressure, Pa, the value is 101325 Pa;
h — the height of the liquid level above the leak, m, taking $h = 0$ m.

Substituting the values of each parameter into formula (6), we can get:

$$Q_m = 1.71 \text{ kg/s}$$

3. Fire simulation

3.1. Modelling

In this paper, geometric modelling of the crude oil generators is built in the SCDM module of ANSYS, which is saved in .obj format. Then the .obj file is translated into a .kfx file, which can be identified by KFX software [17]. Therefore the .kfx file of the geometric model of the crude oil generator room could be imported into KFX software for the next grid division. The number of grids in the model is 30408. The model of the crude oil generator room is shown in Fig. 2.

The ambient temperature of the generator room is 20°C, and the surface temperature of the exhaust hood is about 137°C. Crude oil splatters on the surface of the exhaust hood and burns when heated, which can be simulated approximately according to the pool fire model. The fire area of the pool is 0.88×0.6 m^2, and the depth of the liquid pool is 5 mm. According to the timeline of the accident, the crude oil leakage time was 0 s, and the fire lasted 232 s when the smoke from the exhaust hood was taken as the starting point of the fire, and the simulation time was set to 240 s.

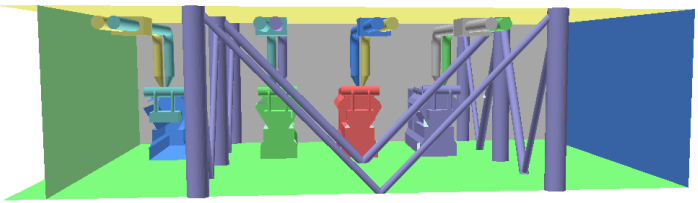

a) Modelling of crude oil generator

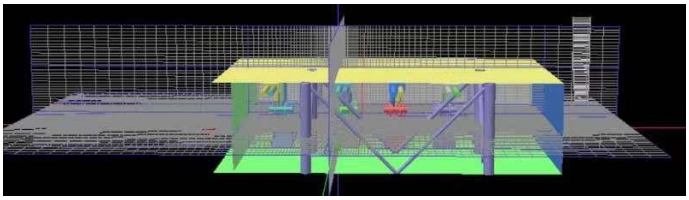

b) Grid of geometric model

Fig. 2. Model of crude oil generator room

3.2. Verification

According to **CCTV** feedback at the scene of the accident, smoke appeared at the front end of the exhaust hood at 12 s and 23 s after the leakage. Compare the simulated situation of the model diagram with the screenshot of the on-site monitoring video at the same time, as shown in Fig. 3.

MATLAB was used to extract the grey values of the two images and normalised them. The results are shown in Fig. 4.

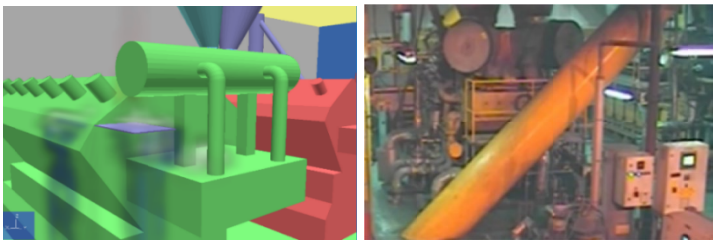

(a) t = 12 s simulation picture (b) t = 12 s **CCTV** picture

(b) t = 23 s simulation picture (c) t = 23 s **CCTV** picture

Fig. 3. Comparison of fire pictures

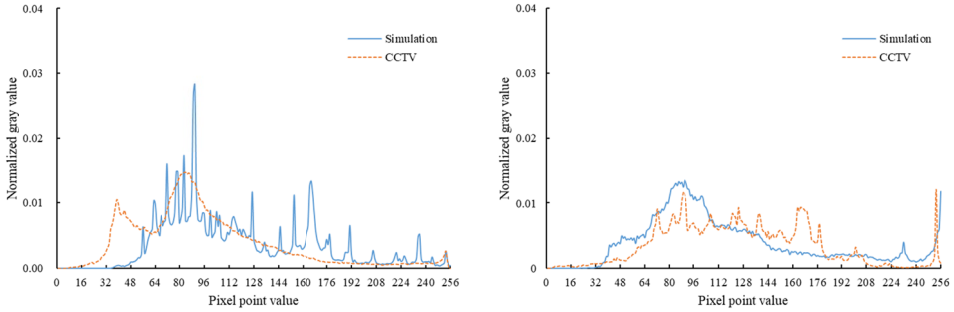

Fig. 4. Similarity analysis of camera and simulation pictures

According to the results of Fig. 4, the grey values of CCTV video images and KFX simulation images at 12 s and 23 s showed the same trend, with good curve coincidence. The similarity of the two images was 85.2% and 90.9%, respectively, with high similarity. It can be seen that the KFX simulation results have good accuracy.

3.3. Simulation analysis of fire consequences

3.3.1. Flue gas volume change

The migration and distribution of smoke in a fire have a prime effect on visibility, which directly affects the success rate of evacuation. The smoke volume rendering of the room at different times is shown in Fig. 5.

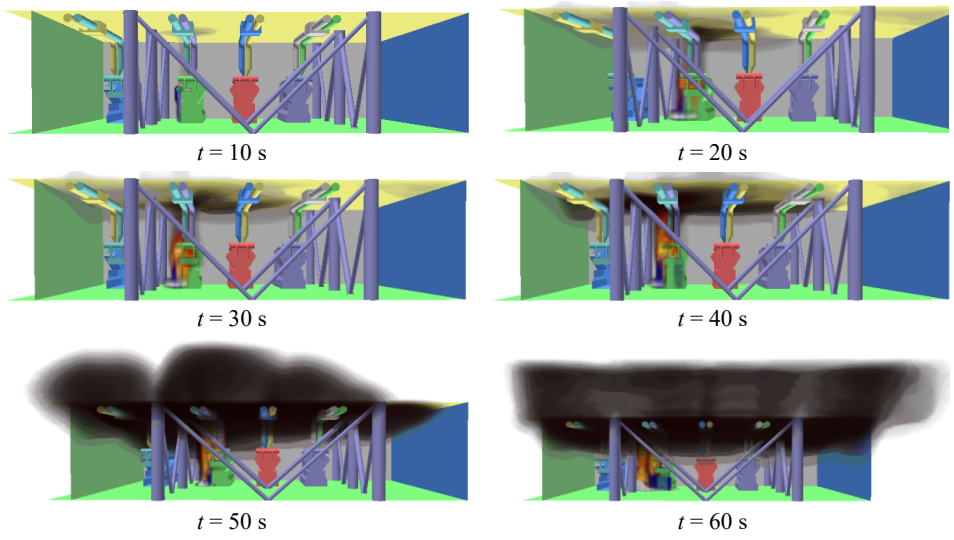

Fig. 5. Smoke volume rendering at different time

As visible in Fig. 5, after the oil leakage is injected into the exhaust hood, it is heated to the flash point quickly and begins to smoke and burn. When t =10 s, as time went on, the fire got bigger and bigger, producing more and more smoke. Smoke gathered at the top of the room and gradually expanded in a circular distribution in time until it spread to the whole oil generator room. The thickness of flue gas was also increased and tended to be stable at about 60 s.

3.3.2. Temperature distribution change

Fig. 6 shows the temperature distribution at different times at the section of the oil generator C fire position.

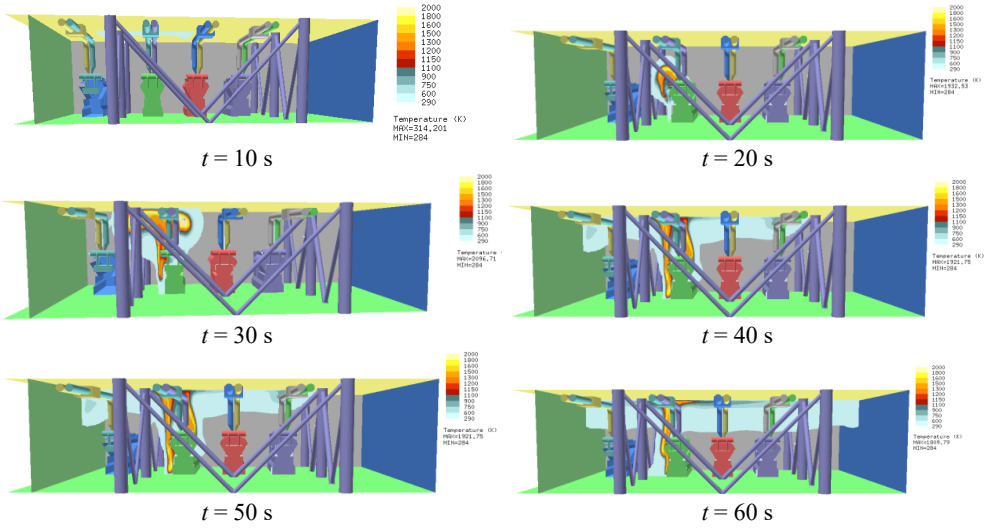

Fig. 6. Temperature contour map of fire section at different time

Strength and deformation recovery of steel depend on temperature for some time after the fire since the offshore platform is a steel frame construction and the top and lower plywood, support, and other elements of the crude oil generator room are made of steel. In general, as long as the temperature does not exceed the abnormal temperature of steel (720 ~ 733°C), that is, within 600°C, it can be considered safe, and its strength and deformation can be restored to the state before the fire [18]. Fig. 6 shows that after t = 30 s, the temperature at the ceiling and flooring of the fire has exceeded 600°C and formed a stable temperature distribution, posing a threat to the strength and deformation recovery of the upper and lower splints and surrounding steel supports. At the same time, the flame has reached a temperature of more than 1,000 degrees Celsius and has begun to spread around the top.

3.3.3. Variation of heat flux

Fire heat radiation can cause serious casualties and equipment damage. The target becomes damaged when the heat radiation flux received by it exceeds or equals the critical heat radiation

flux destroyed by damage, as stated in the formula below (7) [19].

$$q'' \geq q''_{cr} \tag{7}$$

Where:

q — the heat radiation flux received by the target, kW/m^2;

q_{cr} — the critical heat radiation flux for personal injury and equipment damage under the action of steady-state fire heat radiation, kW/m^2.

The heat radiation guidelines for personal injury and equipment damage are shown in Table 1 [20].

TABLE 1

Damage caused by different heat flux

Heat flux/(kW/m^2)	**Damage to equipment**	**Harm to personnel**
35.0-37.5	Equipment was severely damaged	100% death/1 min 1% death/10 s
25.0	The minimum energy required for burning wood under long-term radiation and no flame; the steel structure of the equipment begins to deform.	100% death/1 min Major injury/10 s
12.5-15.0	The minimum energy required to melt plastic and the wood starts to burn with flames; plastic pipes and synthetic materials are melted.	1% death/1 min The burning rate within 10 seconds is 1%
4.0-4.5	Glass breaks after 30 min exposure	Pain over 20 s but no blisters
1.6	—	Long-term exposure to radiation does not cause adverse effects.

According to the heat flux damage and failure criterion, the critical value of heat radiation flux in the above table is 12.5 kW/m^2 (melting of plastic pipe and synthetic material, which can be regarded as the critical value of surface coating damage), 25 kW/m^2 (equipment and steel structure begin to deform) and 35 kW/m^2 (equipment is seriously damaged), and the equivalent surface at a different time at 5.0 m high is taken respectively, See Fig. 7, Fig. 8 and Fig. 9.

As shown in Fig. 7, as time goes by, the volume of the iso-surface with a thermal radiation flux of 12.5 kW/m^2 keeps increasing, mainly because of the continuous leakage and combustion of crude oil and the continuous release of heat. When t = 20 s, the equivalent surface with a thermal radiation flux of 12.5 kW/m^2 surrounds the crude oil generator B and begins to extend to the standby generator C. When t = 50 s, the equivalent surface with a thermal radiation flux of 12.5 kW/m^2 surrounds the crude oil generator C, which will destroy the coating material on the surface of the crude oil generator C and may cause a new fire.

As shown in Fig. 8, the volume of the iso-surface with a thermal radiation flux of 25 kW/m^2 keeps increasing over time. When t = 30 s, the iso-surface of heat radiation flux of 25 kW/m^2 surrounds the left side of crude oil generator B and begins to extend to crude oil generator A. Meanwhile, the iso-surface extends to the top of the generator room and surrounds the support. When t = 50 s, the iso-surface with a heat flux of 25 kW/m^2 surrounds the crude oil generator B and extends to the crude oil generator A. According to the heat flux criterion, when the heat flux reaches 25 kW/m^2, the steel structure of the equipment begins to deform. At this time, the

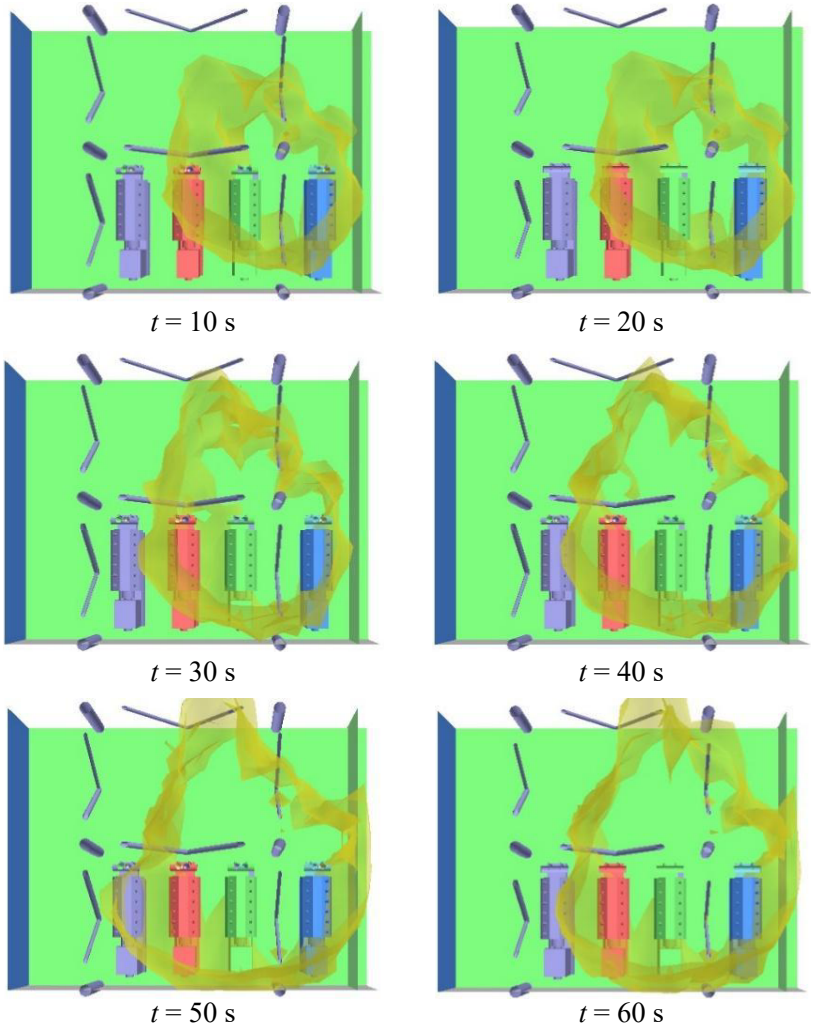

Fig. 7. Isosurface of 12.5 kW/m^2 heat flux at different time at 5.0 m high

steel support inside the crude oil generator room and the top are within the scope of influence. On the one hand, a necessary fire resistance design should be made for these key parts to improve their fire protection grade. On the other hand, after the end of the fire, it is necessary to check the strength of the key support parts to check whether they can meet the strength requirements of the design specifications.

As shown in Fig. 9, the volume of the iso-surface with the thermal radiation flux of 35 kW/m^2 keeps increasing over time. When t = 30 s, the isosurface has expanded to the top of the crude generator room and has mostly encircled the crude generator B. When t = 40 s, the isosurface begins to expand to the backup generator C, penetrating the ceiling and the surrounding region, growing larger and expanding to machine C along the top of the room. According to the heat flux

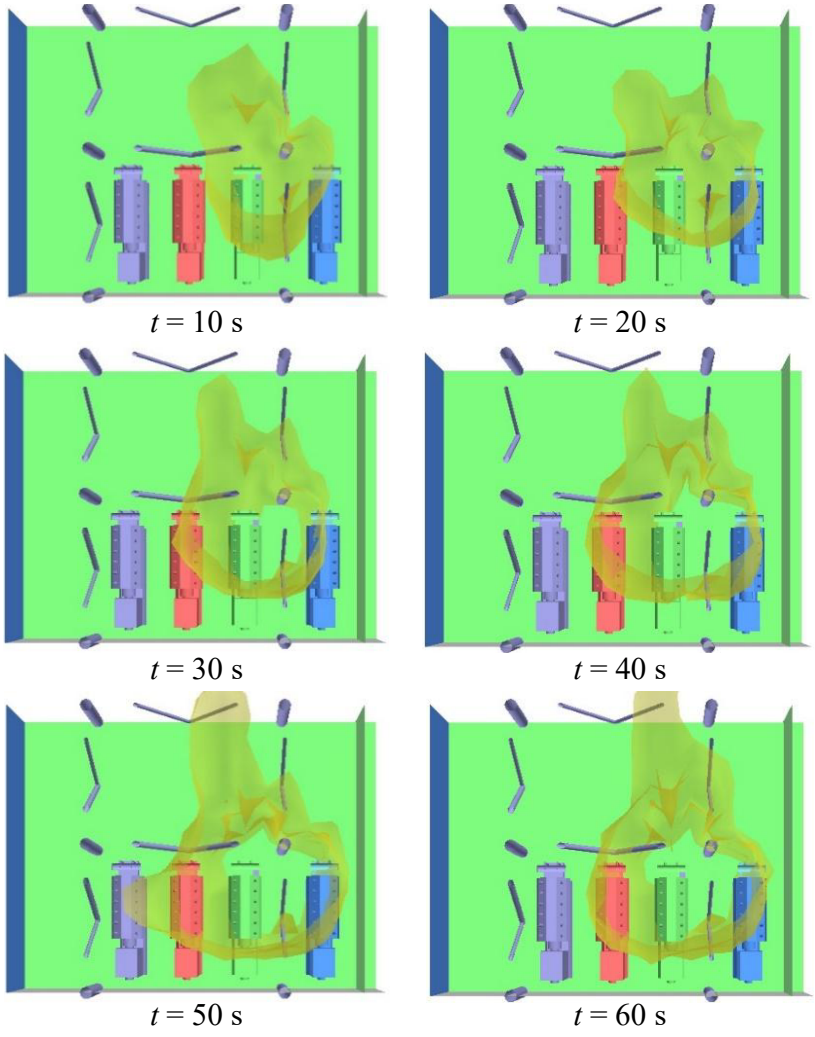

Fig. 8. Isosurface of 25 kW/m^2 heat flux at different time at 5.0 m high

criterion, when the heat flux reaches 35 kW/m^2, the equipment is seriously damaged. It is evident that the thermal radiation intensity of the roof of crude oil generators B and C both exceeds 35 kW/m^2, reaching the condition of significant damage to the equipment and facilities.

4. Fire effects on adjacent devices

High temperatures will affect the strength and deformation of steel structures, posing a threat to the structural stability of offshore platforms. In general, it is believed that steel can be considered safe when the temperature is less than 550°C, and its strength and deformation can be

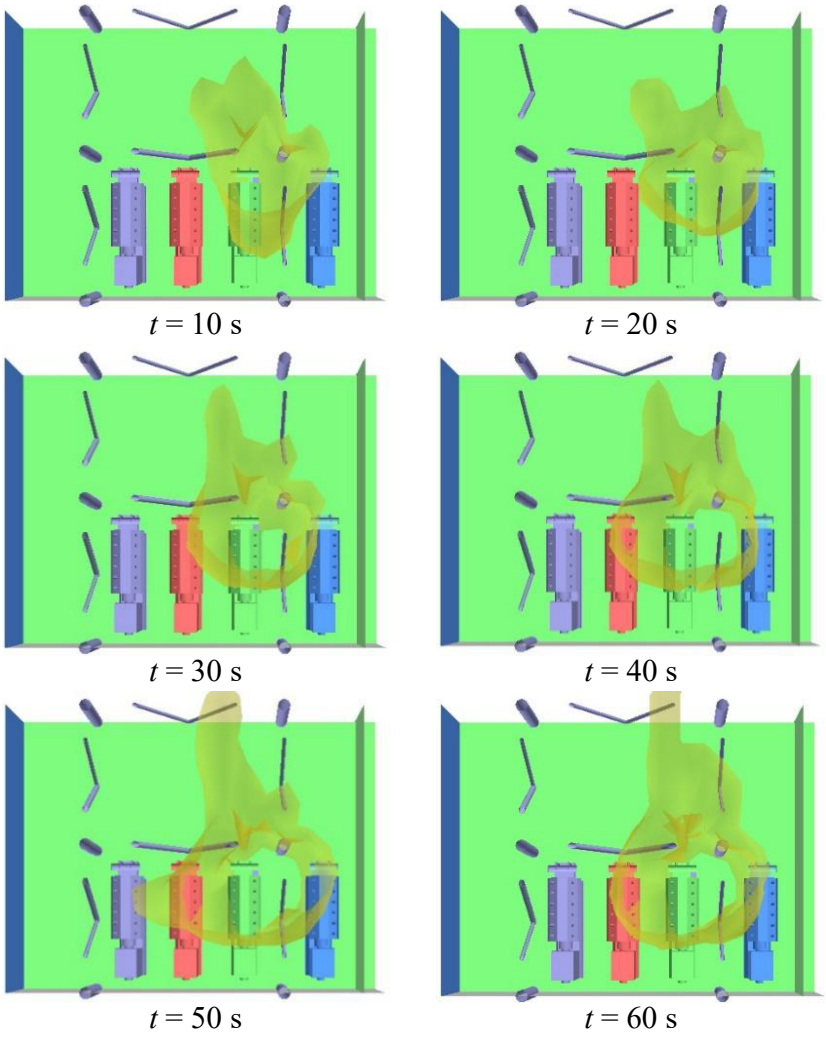

Fig. 9. Isosurface of 35 kW/m^2 heat flux at different time at 5.0 m high

restored to the state before the fire [15]. As the deck and support of offshore platforms are all made of steel, the strength and deformation recovery after a fire depends on the temperature. As a result, the generator room's steel support's temperature change characteristics will be examined.

4.1. Temperature variation of adjacent device

4.1.1. Temperature variation characteristics of steel bracing

This study focuses on steel bracing 1, 2 and 3. According to the simulation results, the temperature change curve is extracted, as shown in Fig. 11.

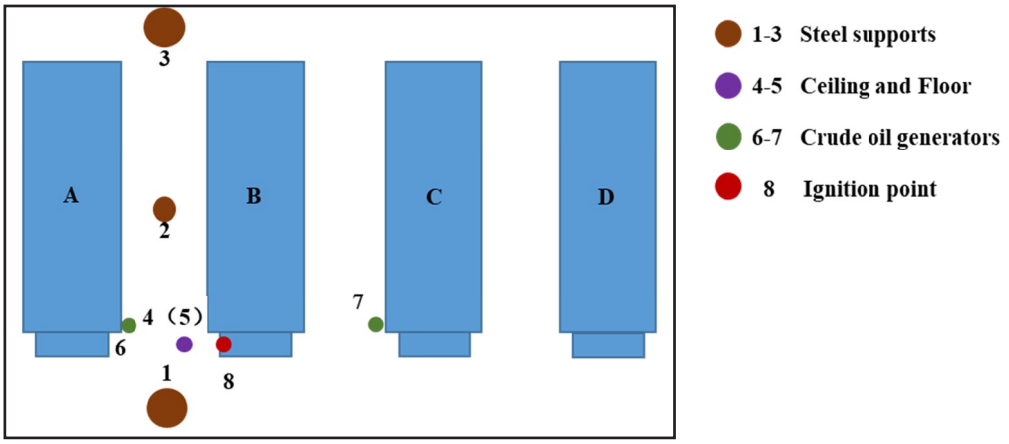

Fig. 10. Layout of nearby position

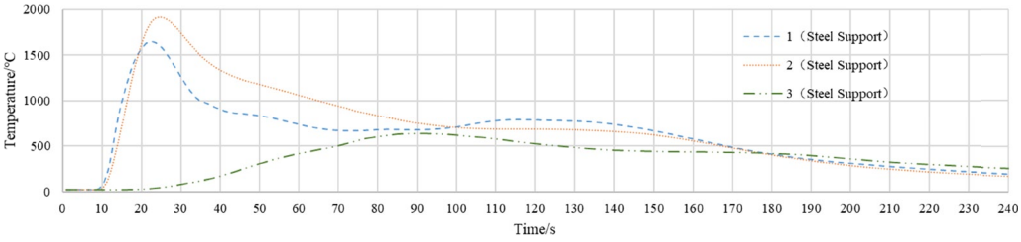

Fig. 11. Temperature contour map of pool fire section at different time

As shown in Fig. 11, the temperature of the steel-supported surface firstly increases, then decreases, and gradually keeps constant. Because the distance between the steel support and the ignition point is different, the maximum temperature, time point of maximum temperature and temperature fall time are different. At about 14 s, steel supports 1 and 2 begin to rise rapidly, and at about 23 s, temperatures peak at 1625°C and 1915°C, respectively. At about 160 s, the temperature of steel support 1 and steel support 2 drops to 600°C. Overall, the fire has posed a threat to the strength and deformation recovery of steel support 1 and 2, lasting about 150 s. For steel support 3, the surface temperature increases first and then decreases. When t = 74 s, the temperature reaches 600 s, while at 90 s, the maximum temperature is about 650°C. It is evident that the temperatures of steel support 1, 2 and 3 all exceeded 600°C and lasted for a period of time.

4.1.2. Temperature variation at the ceiling and flooring

In this study, the heating at the ceiling and flooring of the ignition point was concerned. According to the simulation results, the temperature change curve is extracted, as shown in Fig. 12.

As evident in Fig. 12, the temperature at the ceiling of the ignition location first increases and then decreases, reaching the maximum temperature of 2299°C around 24 s, and then slowly

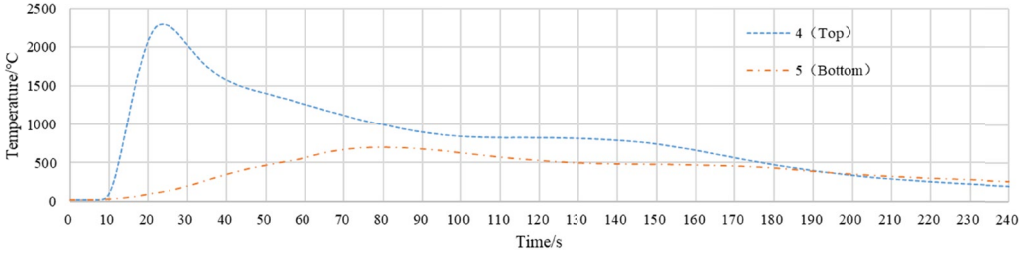

Fig. 12. Temperature of ceiling and flooring of pool fire section at different time

decreases. The temperature at the flooring of the ignition point increases slowly at first and then decreases slowly over time. When t = 63 s, the temperature reaches 604°C. When t = 79 s, the maximum temperature is 701°C. It is evident that the temperature at the ceiling and flooring of the generator room exceeded 600°C and lasted for some time, and the steel material may have irreversibly deformed.

4.1.3. Generator temperature variation

It is necessary to study the temperature variation characteristics of the adjacent crude oil generator because it may cause internal damage due to high temperature. Here, temperature changes of adjacent points of original generator **A** and crude oil generator **C** are extracted, as shown in Fig. 13.

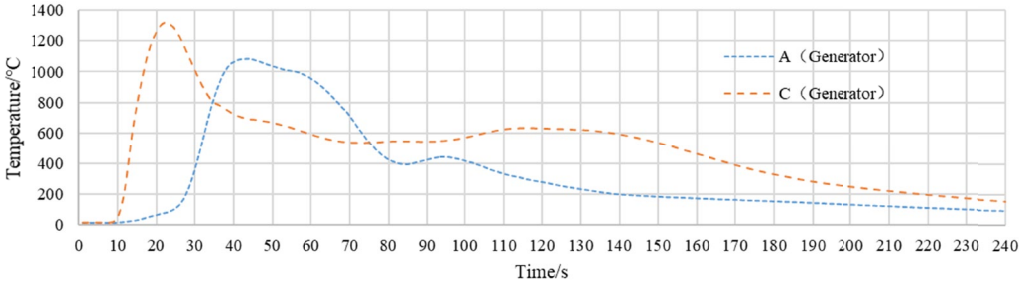

Fig. 13. Temperature variation in the position of oil generator

As evident in Fig. 13, the temperature at the adjacent point of generator **A** first increases and then decreases, and then gradually decreases and tends to be stable. When t = 14 s, the temperature reaches 641°C, and When t = 24 s, the maximum temperature reaches 1299°C. The temperature near the crude oil generator **C** increases first and then decreases with time, and then tends to be stable. When t = 33 s, the temperature reaches 656°C. When t = 44 s, the maximum temperature is 1085°C. It is clear that there is a possibility of high temperature melting at the inlet hose **C** and the risk of further oil leakage.

4.2. Heat flux variation of adjacent devices

4.2.1. Heat flux of steel support

In this study, the heat flux of steel supports 1, 2 and 3 are mainly concerned. According to the simulation results, the change curve of thermal radiation flux is extracted, as shown in Fig. 14.

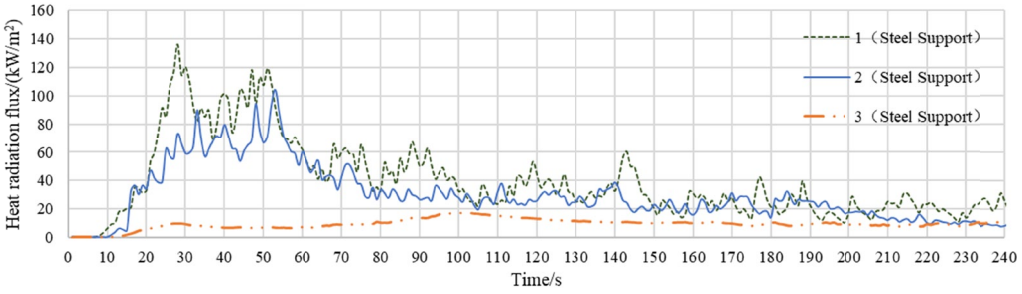

Fig. 14. Radiation at steel supports

As evident from Fig. 14, the heat radiation flux from steel support increases first and then decreases to a certain value with time. It is apparent that for steel support 1, the maximum thermal radiation is 136 kW/m^2 When t = 28 s, and the final floating value is 20 kW/m^2. Steel supports 2 and 3 reach their maximum values of 104 kW/m^2 and 17 kW/m^2 When t = 53 s and 99 s, respectively, and finally float at 14 kW/m^2 and 12 kW/m^2. As shown in Table 1, when the heat radiation flux reaches 37.5 kW /m^2, the steel structure begins to deform and fail. Therefore, it is clear from the figure above that the heat radiation values of steel support 1 and 2 all exceed 37.5 kW /m^2, which meets the condition of severe damage to the steel.

4.2.2. Heat flux at ceiling and flooring

Heat flux at the ceiling and flooring of the main ignition points in this study. According to the simulation results shown in Fig. 15, the change curve of thermal radiation flux is extracted.

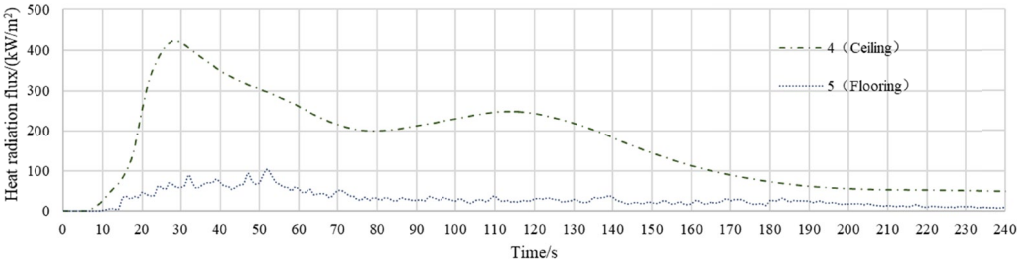

Fig. 15. Radiation at ceiling and floor

As evident from Fig. 15, the heat radiation flux at the ceiling and floor of the ignition point increases first and then decreases to a certain value with time. For the top of the ignition point, the maximum thermal radiation is 422 kW/m^2 When t = 28 s, and the final floating value is 50 kW/m^2. At the bottom of the ignition point, the maximum thermal radiation is 104 kW/m^2 when t = 52 s, and the final floating value is 5 kW/m^2. As shown in Table 1, the steel structure begins to deform when the heat radiation flux reaches 25 kW/m^2. Therefore, it is clear from the figure above that the heat flux at the ceiling and floor of the generator room both exceeds 25 kW/m^2, which meets the condition of steel deformation.

4.2.3. Heat flux of adjacent generators

According to the simulation results, the thermal radiation flux at the adjacent points of oil generators A and C is extracted, as shown in Fig. 16.

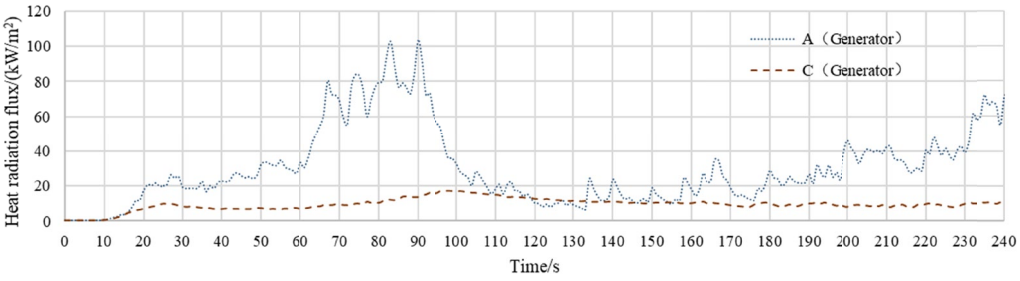

Fig. 16. Radiation at adjacent oil generator **A** & **C**

It can be seen from Fig. 16 that the thermal radiation flux near the point of crude oil generator A first increases and then decreases to A certain value. When t = 10 s, the heat flux near generator A begins to increase rapidly, and When t = 90 s, the heat flux reaches 105 kW/m^2. The heat flux near the crude oil generator C increases slowly and then decreases to a certain value, and the heat flux never exceeds 20 kW/m^2. According to Table 1, when the heat radiation flux reaches 25 kW/m^2, the steel structure of the equipment reaches the condition of deformation. It is evident that oil generator A has the possibility of structural deformation, which requires further internal inspection after the disaster, while oil generator C does not have the condition of structural deformation.

5. Conclusions

Based on the background of a generator fire accident on an offshore platform, the variation characteristics of temperature and thermal radiation parameters near the key components, such as steel supports and oil intake hoses, were studied by numerical simulation, and the following conclusions are drawn:

(1) After the leaking oil is injected into the exhaust hood, it is quickly heated to the flash point and begins to smoke and burn. In less than a minute, the smoke can spread throughout

the room. The thickness of the smoke increases, directly reducing the success rate of evacuation.

(2) Adjacent steel support 1 and 2 reach the conditions of deformation and failure. The ceiling and flooring of the oil generator room reach a condition of significant damage. The crude oil generator A and C reach the condition of serious damage.

(3) According to the spatial and temporal variation characteristics of temperature and heat radiation flux of adjacent fire equipment and facilities, it can provide a reference for the arrangement of flame detectors in adjacent areas and the strength check of post-disaster equipment and facilities structure.

Reference

[1] X.F. Song, J.H. Lu, An overview of pool fire models applicable to offshore platforms. Petroleum Engineering Construction **37** (2), 1-5, 83 (2011).

[2] Z.S. Luo, J.C. Xu, N.N. Zhang, Analysis of thermal radiation hazard of fire disaster based on offshore oil and gas platforms leakage. Fire Science and Technology **35** (1), 6-10 (2016).

[3] X.F. Song, Structural analysis of a jacket platform on fire. Ocean University of China. 2011.

[4] T. Hu, Research on the fire control system design of organic liquid storage tank area. master thesis. Southwest Petroleum University. 2015.

[5] J. Guo, Y. Zhu, G. Chen, Fire hazard analysis on oil & gas processing systems on the offshore platform based on FDS. China Offshore Oil and Gas **23** (2), 126-130 (2017).

[6] C.Y. Chen, Numerical simulation of fire heat flow field and evacuation analysis in an ocean platform. Master thesis, Jiangsu University of Science and Technology. 2018.

[7] F. Tong, Y.N. Xiang, H. Shen, Temperature field and structure response of offshore platform room under local fire. Urbanism and Architecture **18** (403), 130-132 (2021).

[8] T.X. Niu, K.Q. Zhu, Y.F. Mao, Analysis of FPSO pool fire. Ship Engineering **39** (9), 64-70 (2017).

[9] J.Y. Yoon, S.H. Kim, G.C. Yu, Effects of wind on the heat flow of FPSO topsides subject to fire: an experimental and numerical study. ASME 2010 International Conference on Ocean 949-958 (2010).

[10] X.L. Xie, Y. Zhu, Z.Y. Zhang, et al. Performance evaluation and improvement for fire protection systems of FPSO pump cabins. China Offshore and Gas **29** (4), 175-181 (2017).

[11] G.H. Xu, esearch on the fire risk assessment and simulation of generator room in the offshore oil platform. Master thesis, South China University of Technology. 2017.

[12] D.P. Yang, G.M. Chen, C.Q. Niu, etc. Simulation and evaluation of oil and gas fire accidents on the shallow sea platform. Safety Health & Environment **19** (1), 19-25 (2019).

[13] Y.L. Chen, Further development of the eddy dissipation model for turbulent non-premixed flame. Xiamen University 2020.

[14] S.Y. Ge, H.Y. Na, Thermal radiation properties and measurement. Beijing, Science Press 1989.

[15] J.D. Yao, W.C. Fan, Theory and numerical simulation of 3D discrete transfer radiation model. Journal of Combustion Science and Technology (3), 264-267 (1995).

[16] Y.D. Shi, The simulation analysis on buried pipeline fire consequence. Safety Health & Environment **16** (3), 21-24 (2016).

[17] DNV-GL. KFX-EXISM V.3.4 User Manual, Technical Manual; DNV-GL: Berum, Norway, 2019.

[18] E.F. Du, Experimental and theoretical research on the structural behavior of large space steel structures subjected to natural fires. Master thesis, Southeast University 2016.

[19] Z.M. Fu, J.Y. Huang, M. Fu, Quantitative analysis of the radiation damaging effects caused by liquid or gaseous hydrocarbon fires. China Safety Science Journal (9), 29-36 (2008).

[20] AQT. Guidelines for quantitative risk assessment of chemical enterprises. 3046 (2013).